HHS Public Access

Author manuscript

Sens Actuators B Chem. Author manuscript; available in PMC 2018 March 31.

Published in final edited form as:

Sens Actuators B Chem. 2017 March 31; 241: 398–405. doi:10.1016/j.snb.2016.10.079.

Local pH Monitoring of Small Cluster of Cells using a Fiber-Optic Dual-Core Micro-Probe

Sisi Chen[1,3], **Qingbo Yang**[1,3], **Hai Xiao**[2,3], **Honglan Shi**[1,3], and **Yinfa Ma**[1,3,*]

[1]Department of Chemistry, Missouri University of Science and Technology, Rolla, MO, 65409, USA

[2]Department of Electrical and Computer Engineering, Clemson University, Clemson, SC, 29634, USA

[3]Center for Single Nanoparticle, Single Cell, and Single Molecule Monitoring, Missouri University of Science and Technology, Rolla, MO, 65409, USA

Abstract

Biological studies of tissues and cells have enabled numerous discoveries, but these studies still bear potential risks of invalidation because of cell heterogeneity. Through high-accuracy techniques, recent studies have demonstrated that discrepancies do exist between the results from low-number-cell studies and cell-population-based results. Thus the urgent need to re-evaluate key principles on limited number of cells has been provoked. In this study, a novel designed dual-core fiber-optic pH micro-probe was fabricated and demonstrated for niche environment pH sensing with high spatial resolution. An organic-modified silicate (OrMoSils) sol-gel thin layer was functionalized by entrapping a pH indicator, 2′, 7′-Bis (2-carbonylethyl)-5(6)-carboxyfluorescein (BCECF), on a ~70 μm sized probe tip. Good linear correlation between fluorescence ratio of $I_{560\ nm}/I_{640\ nm}$ and intercellular pH values was obtained within a biological-relevant pH range from 6.20 to 7.92 ($R^2 = 0.9834$), and with a pH resolution of 0.035 ± 0.005 pH units. The probe's horizontal spatial resolution was demonstrated to be less than 2mm. Moreover, the probe was evaluated by measuring the localized extracellular pH changes of cultured human lung cancer cells (A549) when exposed to titanium dioxide nanoparticles (TiO_2 NPs). Results showed that the probe has superior capability for fast, local, and continual monitoring of a small cluster of cells, which provides researchers a fast and accurate technique to conduct local pH measurements for cell heterogeneity-related studies.

Graphical Abstract

*Corresponding Author: Department of Chemistry, Missouri University of Science and Technology, 400 West 11th Street, Rolla, MO 65409, Tel: 573-341-6220, Fax: 573-341-6033, yinfa@mst.edu.

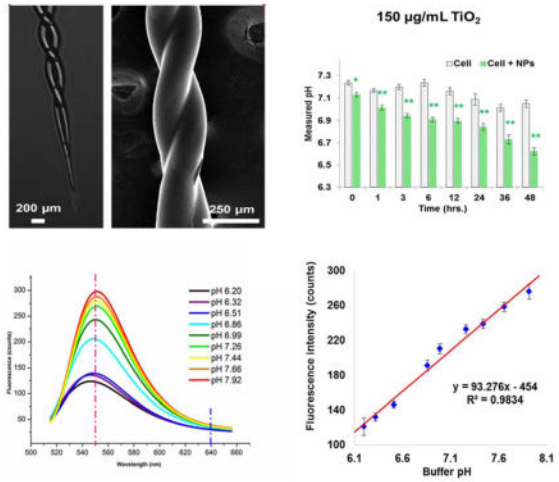

Keywords

pH micro-probe; Fiber-optic sensor; Cell heterogeneity; Local/niche environment sensing; Organic modified silicates (OrMoSils); TiO_2 nanoparticles (NPs) cytotoxicity

Introduction

Tissue and cellular level biological studies have enabled numerous scientific discoveries and biomedical applications. However, potential risks still exist when cell heterogeneity is taken into consideration, which may invalidate some of the fundamental principles that have been established previously [1–3]. The recent data generated by new high-accuracy techniques indicate that discrepancies do exist among those cell-population based results [4–7], and thus there is an urgent need to re-evaluate some essential parameters with limited number of cells in order to truly realize precise medicine in the future.

The intra-/inter-cellular pH, as one of such key parameters, plays a key role in many cell behaviors and responses to surrounding stimuli [8]. The pH in cytosol and nucleus is normally adjusted to 7.2–7.4, and to 4.0–5.5 in endosomes and lysosomes [9, 10], and pH dysregulation leads to dysfunction of cells [11–14]. However, it is interesting to note that the intra- and extra-cellular pHs of tumor cells are regulated to be >7.4 and around 6.7–7.1, respectively [15–17], which is quite different from normal cells. These and more examples [18–21] demonstrate the significant roles that pH plays in many cell events. Unfortunately, current available techniques cannot provide the fast and local cellular pH measurements with high spatial resolutions that are necessary to distinguish potential heterogeneity among different cells. Conventional fluorescent dyes, like 2′,7′-bis-(2-carboxypropyl)-5-(and-6-)-carboxyfluorescein (BCPCF) [22] and 2′,7′-Bis (2-carbonylethyl)-5(6)-carboxyfluorescein (BCECF) [17], are commonly used pH indicators, and in most cases they are hydrophobically modified for cytosolic but not for extracellular sensing. Particle-based nano-sensors, a new type of pH sensors, which can be embedded with Oregon Green (OG) and fluorescein, have been reported [23–25]. However, their potential toxicity of nanostructures to cells is still a problem for real time pH measurements while cells are still

functioning. Other pH measurement approaches, such as fluorescence resonance energy transfer (FRET) based probes [26] and ion-sensitive field-effect transistor (ISFET) based sensors [27, 28], encounter more or less complexity and difficulties in their detecting principles and/or fabricating processes. In addition, dealing with toxic heavy metal elements during probe development and manufacturing is also a concern in semiconductor-based approaches.

Fiber-optic-based sensors have been developed that are easy to fabricate, quick to respond, able to provide high spatial resolution detection, and have minimum invasiveness to cells [29–32]. A unique way of making fiber-optic-based pH sensors has been reported by using sol-gel coating techniques [33]. The novel point in using a sol-gel derived thin layer is that its nano- to micro-scale porous structure of the solidified networks can effectively entrap the pH indicating molecules. Furthermore, formed aerogel has high thermal stability and optical transparency, and is feasible for direct coating onto glass substrates [34].

In this study, a newly designed dual-core double-fiber twisted pH probe for quick fabrication and application was successfully fabricated and validated for niche cellular environment pH monitoring. The dual-core double-fiber configuration was fabricated by using a home-built twisting and gravitational-stretching system. A semi-spherical head design was applied in the new probe for maximum fluorescence reflection and collection, and the new probe head design was achieved by a distant fusion splicing method. Again, the pH sensitive dye BCECF was used and covalently entrapped in an organic-modified silicate (OrMoSils) sol-gel thin layer that was coated onto the sensing-head surface. The follow up scanning electron microscopic (SEM) imaging and energy-dispersive spectroscopy (EDS) characterization showed the successful fabrication of this probe, and probe validations in both standard pH buffers and cultured human lung cancer cells that were exposed to TiO_2 nanoparticles (NPs) were conducted in order to demonstrate the probe's applicability in many potential biomedical research areas.

Materials and Methods

Fabrication and coating of micro-pH probe

The dual-core micro-pH probe with a semi-spherical head shape was fabricated from two single mode optical fibers with core and cladding diameters of 62.5 and 125 μm (Corning, MA) using a homemade twisting and gravitational-stretching system (Fig. 1a). The cores of two optical fibers were fused with an optical fiber fusion splicer (Fujikura, Japan). In order to minimize background noise, one of the optical fibers served as an excitation laser transmission while the second fiber was used for fluorescence light collection. The pH-sensitive fluorescent dye 2′, 7′-Bis (2-carbonylethyl)-5(6)-carboxyfluorescein (BCECF) (LifeTechnologies Inc., New York) was mixed with an ultra-thin aerogel layer for pH sensing. The sol-gel dip-coating procedure was similar to our previous study [35, 36]. The chemicals used for coating, including dimethyl sulfoxide (DMSO), 2-succinimido-1,1,3,3 tetram-ethyluronium tetrafluoroborate (TSTU), N-ethyldiisopropylamine (Hünig's base), (3-Aminopropyl) triethoxysilane (APTES), tetraethoxysilane (TEOS), methyltrimethoxysi-lane (MTES), were purchased from Sigma-Aldrich (St. Louis, Missouri). The probe was acidified with concentrated nitric acid for 12 hours and washed with sufficient amount of Mili-Q

(MQ) (EMD Millipore Corp., MA) water and pure ethanol. The probe was then dried at 100 °C for at least 3 hours. An alkoxides mixture was prepared with APTES, TEOS and MTES at a ratio of 4:1:1 (v/v) with catalytic amount (2% of total volume) of hydrochloric acid (0.1 M). The dried probe was dipped into the alkoxides mixture with a drawing rate of ~1 mm/s, and this process was repeated 8 – 10 times to obtain a sufficiently thick layer after curing. The mixture of BCECF, TSTU, and Hünig's base was reacted for one hour at room temperature. The probe was then dipped into the dye solution for about 20 minutes and was incubated for 6 hours at 50 °C and then another 24 hours at 80 °C.

Characterization of micro-pH probes

The coated dual-core micro-pH probes were imaged by an inverted fluorescent microscope (Olympus IX51, Olympus, center valley, PA, USA) and scanning electron microscopy (SEM). The thin layer of coating on the probe's tip was characterized by energy-dispersive X-ray spectroscopy (EDS) (FEI, Hillsboro, OR, USA), including five scanned elements, carbon (C), nitrogen (N), oxygen (O), silicon (Si) and gold (Au). An inverted fluorescent microscope was used to take images of the probe under white light and an FITC fluorescent channel, with which the BCECF dye can be examined. A quick-dry epoxy resin (EpoHeat, Buehler, Illinois) was used to embed the finished probes into the solidified resin, followed by cross-sectioning and fine grinding to just expose the probe head.

The pH probe was excited by a 488 nm continuous-wave (CW) Argon ion laser source (Spectra-Physics Lasers, Mountain View, California, USA), and a USB2000 spectrometer (Ocean optics, Dunedin, Florida) was used to collect the fluorescent signals at 560 nm. Before use, each fabricated probe was calibrated with a series of standard pH buffer solutions, which were prepared in 0.1 M phosphate buffer solution (PBS) (Life Technology, New York, USA). The pH values of the standard buffer solutions ranged from 5.86 to 8.45 with pH intervals around 0.2 that were first calibrated with Accumet AB15+ pH meter (Fisher Scientific, Pittsburgh, PA, USA). Afterwards, the coated dual-core double-fiber-twisted pH probe was dipped into pH solution for 15 ± 5 seconds to obtain a stable fluorescence reading, and the fluorescent spectrum was acquired. The probe was then rinsed with a sufficient amount of MQ water before the next measurement was conducted.

TiO_2 nanoparticles and characterization

The TiO_2 nanoparticles with sizes of 30 – 50 nm were purchased from Sigma-Aldrich (St. Louis, Missouri). The suspension of TiO_2 was prepared in cell culture medium without serum and sonicated 15 minutes by an ultrasonicator (FS-60H, 130W, 20 kHz; Fisher Scientific, Pittsburg, PA, USA). The TiO_2 nanoparticles were imaged and characterized by transmission electron microscopy (TEM) and EDS.

Spatial resolution test of micro-pH probe

TiO_2 NPs were measured 3.5 mg in total, and were slowly dosed directly onto one single point (diameter < 1mm) at the bottom of a dish that was pre-cultured with A549 cells. The pH of three different local points in the same dish, at distances from the NP-dosing spot of 0 mm, 2 mm and 10 mm, were continuously monitored using our probe for 4 hours.

Meanwhile, a separate dish that was also dosed with same amount of TiO_2 NPs but without cell cultures was also monitored to evaluate pH variation caused by NPs.

Cell culture conditions and treatment with TiO_2

The adenocarcinomic human alveolar basal epithelial cell line, A549, was obtained from American Type Culture Collection (ATCC) (Manassas, Virginia). Ham's F-12K medium with L-glutamine was purchased from Caisson Laboratories (North Logan, Utah), and was supplemented with 2 mM L-glutamine, 1 mM sodium pyruvate, 1% non-essential amino acids, 50 U/mL penicillin, and 50 mg/mL streptomycin for sub-culture. Cells were cultured at 37 °C with 5% CO_2 and 95% humidity. A549 cells were pre-seeded into a 96-well plate (Corning Inc., New York) at a density of 1×10^5 cells per well in 200 μL culture medium and cultured for 16–18 hours to allow cells to attach. Different concentrations (50, 100 and 150 μg/mL) of TiO_2 NPs suspensions were prepared separately with Ham's F-12K medium and immediately applied to the cells after pretreatment. Cells without NPs treatment served as controls in each experiment. The pH reactive oxygen species (ROS) generation, and cell viability were all measured after 0, 1, 3, 6, 12, 24, 36, and 48-hour exposures to the nanoparticles.

pH measurement of cell colony

The coated dual-core micro-pH probes were applied to measure the pH of the micro-environment around the cells treated with different concentrations of TiO_2 nanoparticles. After exposure to different concentration of TiO_2 nanoparticles for 1, 3, 6, 12, 24, 36, and 48 hours, the probe was dipped into each well to conduct a pH measurement. After each measurement, the probe was rinsed with sufficient amounts of MQ water.

Assessment of cytotoxicity

To determine the cytotoxicity of TiO_2 nanoparticles, the cell proliferation reagent WST-1 (Roche Life Science, Indianapolis, Indiana) was used following the manufacturer's instructions. After cells were exposed to TiO_2 nanoparticles for 1, 3, 6, 12, 24, 36, and 48 hours, the absorbance at 450 nm was measured using a microplate reader (FLOURstar; BMG Labtechnologies, Durham, North Carolina).

The ROS level was determined by using Penicillin–streptomycin, 2′, 7′ - dichlorofluorescin diacetate (DCFH-DA) purchased from Life Technology (Grand Island, New York). The stock solution was prepared in dimethyl sulfoxide (DMSO) at a final concentration of 10 mM and the 20 μM working solution was prepared by diluting the stuck solution 500-fold with Hanks' Balanced Salt solution (HBSS, Life Technology, Grand Island, New York). The supernatant was taken out from each well, and cells were incubated with the working solution in a dark environment for 1 hour at 37 °C. Fluorescence was then determined at 485 nm excitation and 520 nm emission using a microplate reader (FLOUR star; BMG Lab Technologies, Durhan, North Carolina).

Statistics

Experimental data in this study were analyzed by one-way ANOVA followed by a Post Hoc test. All experimental results were expressed as the mean value, and standard deviation (SD)

was derived from triplicate measurements. Two-tail Student's *t*-test was applied for significance testing. The level of statistical significance was presented as a *p*-value of <0.05 (*), <0.01 (**) as well as <0.001 (***).

Results and discussions

Probe Fabrication

Our prior studies [35, 36] have reported the development of micro-spherical and 1-in-6 hexagonal fiber-optic pH sensors, which demonstrate a new approach to measure pH in a confined niche environment, including at the single-cell level. In the present study, the probe structure was redesigned to reduce the difficulty of fabrication and to achieve quick sensing performance (Fig. 1). A twisted fiber configuration provides several advantages over a parallel aligning configuration, such as better robustness and structural uniformity, thus enhancing the light transmission. The gravitational-stretching system provides controllable forces while pulling twisted fibers down to a micro-sized taper (Fig. 1b). A home-built double-fiber twisting and gravitational-stretching system was used for the main sensing stem fabrication (Fig. 1a). Using a pencil flame torch enabled us to precisely fabricate a short length (0.5 – 1.2 cm) twisted sensor shaft with two fibers fused only at the cladding section. A distant-fusion was applied to mildly bend inner cores toward each other with an intermediate thin (<5 μm) layer of cladding (Fig. 1c, 1d). Finally, a sol-gel dip-coating procedure was applied, followed by aging, curing, and carbon dioxide (CO_2) supercritical drying. A covalent bond between pH sensitive dye and the aerogel was thus formed (Fig. 1e), as described in our previous work [35].

The fabricated probe was characterized through SEM/EDS scanning (Fig. 2). Results showed that the fabricated probe head had a diameter of around 80 μm. A cross-section image evidently proved a cladding-only fusion as expected (Fig. 2, a–d). An outside enwrapping layer (3 – 8 μm) (Fig. 2d) around the two inner fibers was the dye embedded aerogel, featured with typical porous networks (Fig. 2e), which allows quick interactions between protons (analytes) and BCECF molecules. EDS scanning showed the existence of high percentages of carbon (20.81%) and nitrogen (6.29%), while considerably low oxygen (67.8%) and silica (4.15%) (Fig. 2f), when compared to non-coated area (Fig. 2g, h), indicating successful amide bonding of BCECF [35]. These overall observations demonstrated a successful fabrication of a dual-core micro-pH probe featured with a BCECF dye-doped aerogel sensing layer.

System setup and probe calibration

The reflection-mode probing system is composed of two major parts, a laser excitation pathway, and a fluorescence signal collection pathway, which are joined together at the sensor tip [37]. Briefly, the 488 nm Argon ion laser beam was introduced into one fiber through focusing, and the excited fluorescence emission can be picked up by the other fiber and transmitted to the detector (Fig. 3a). More detailed procedures can be found elsewhere. Compared to our previous single fiber configuration [35], this design can significantly separate the exciting laser and emission signal light through two-fiber usage and separated cores, thus this design may provide a higher signal-to-noise (S/N) ratio.

The finished probe was then calibrated by a set of stepping pH buffers that were standardized using a conventional pH meter. A fluorescence peak was observed at around 550 nm (Fig. 3b), and the peak intensity was found to be linearly correlated with the pH values. The linear correlation range was observed from pH 6.20 to pH 7.92 with a coefficient factor of 0.9834 (Fig. 3c). Over this pH range, a typical sigmoidal correlation was observed. We thus specifically chose to focus on the linear correlation region, which had already covered the most interested biologically relevant range. Triplicate measurements were conducted for each probe, and several probes were used to come up with a pH detecting resolution of 0.035 ± 0.005 pH units calculated by the standard deviation from triplicate measurements, indicating a good reproducibility. Higher sensitivity and pH resolution can theoretically be further achieved by increasing the dye concentration or the laser power. However, this was not recommended due to the possibility of self-quenching and photo-bleaching [37]. The current methodology may also suffer from varied temperature and ionic strength, as has been discussed elsewhere [35, 36]. Nevertheless, no significant interferences to the probe were observed due to these two factors, as long as the measuring condition fell within a biologically relevant range.

Determination of probing spatial resolution

To validate the detecting spatial resolution of the fabricated probe, we used spot dosing (Fig. 4d) of 30 – 50 nm TiO_2 NPs (Fig. 4, a–c) to induce cell deterioration. Results showed apparent pH decreases in all cells + NP groups, while no significant changes were observed in the NP-only groups. Statistically significant differences between cells + NP and control groups began to show after the 90-minute NP dosing. After 150 minutes, significant differences between cells + NPs groups also started to show (Fig. 4e). The latter results particularly indicated a site difference of cell responses due to the non-evenly distributed NP concentration. The capability to differentiate such small-scale pH values also indicated the high spatial resolution of our probe. This ability is essentialfor site-specific measurement in a local area, and especially when the pH is variated drastically in that niche environment, such as within a small cluster of cells or a wounded tissue area, etc.

Detecting early onset of cell deterioration induced by TiO_2 NPs

To further demonstrate the probe's ability to detect actual cellular events, the probe was applied to monitor cell response to TiO_2 nanoparticles. Engineered nanoparticles (ENPs), though used in many fields such as biomedical imaging and detecting [38, 39], cancer therapy [40], drug delivery [41], water purification [42], and cosmetics [43, 44], bear potential toxic concerns due to their intrinsic nano-scale sizes, heavy metal composition, large specific surface areas, and high photo-reactivity [45–47]. The NP-caused cell damages are hard to track and study because they are complicated and highly spatiotemporally specified. In the present study, both the probe and two conventional methods were used to monitor cell changes in pH, viability, and ROS. An adenocarcinomic human alveolar basal epithelial cell line, A549 (CCL-185, ATCC), was used and a 40 nm sized TiO_2 NPs at concentrations of 50, 100, and 150 μg/mL were applied for cell exposure up to 48 hours. A cell-only group was used as the control in all tests. An NP-only group was also tested and no significant pH variations were induced by the NPs (data not shown).

Results showed decreased pHs and cell viabilities and increased ROS accumulation in NP-dosed groups (Fig. 5). We interpreted these results as an early onset of cell deterioration due to the NP's toxicity, and the down regulation seemed related to this process. In detail, higher NP dosages resulted in lower viability and pH, and higher ROS generation. Meanwhile, no significant pH variation in the control group was observed. A similar result was shown in a previous study where cell apoptosis was correlated with TiO_2 NP's concentration [46]. Additionally, a time effect was also observed: the longer the NPs were exposed, the lower the viability and pH, while the higher the ROS. Compared with the two conventional methods, the pH measurements showed at least equal ability in detecting NP-induced cell deterioration (which statistically differed from the control group). However, at the highest NP-dosing concentration, our probe can effectively differentiate the signals generated by the NP-dosed cells from those of the control cells ($p < 0.05$, "*") when NPs were just applied, which is couple of hours ahead of the statistically meaningful results that were reported by the viability and ROS assays.

The purpose of using two traditional assays, cell viability and ROS generation, was to demonstrate the effectiveness of the pH probe. On one hand, cell viability was reflected by the enzymatic activity of the mitochondrial level of succinic dehydrogenase, which was finally represented by the formazan concentration through a colorimetric evaluation [48]. ROS generation, one of the known NP-induced syndromes [45, 46, 49], has also been correlated with the mitochondrial inner membrane potential [50]. Thus, both viability and ROS assays are related to mitochondrial stability and may serve as relatively early-stage signs of cell deterioration before whole cell degradation occurs. On the other hand, ion channels, such as H^+/K^+, Na^+/H^+, Cl^-/HCO_3-, were also correlated with pH regulation. And these ion channels were found on both cell and mitochondrial membranes [51]. Our results, thus, showed an important correlation between extracellular pH and NP exposure. The detected pH changes featured a locally radical acidification due to the NP destruction, and such local changes happened faster than the other two population-based assays. Although further mechanistic studies on the pH variation triggering points during NP-induced cell degradation and its correlation with mitochondria stability are still needed, our developed pH micro-probes may find applications in detecting subtle and local cellular changes in a fast and stain-free manner.

Conclusions

In this study, we successfully developed and fabricated a novel dual-core micro-pH probe using a home-built double-fiber twisting and gravitational-stretching system. The probe was coated by a specific OrMoSils dye-doping method and applied for pH sensing in a microliter environment. The enhanced mechanical structure of the probe with fused double fibers successfully separated the excitation beam and emission light, thus providing the robust probe with reduced background noise and increased sensitivity. A linear correlation between pH and spectral peak intensity was found within a biologically meaningful pH range of 6.20 to 7.92 and a correlation coefficient of 0.9834 was achieved. The probe's spatial resolution was then exemplarily tested and a resolution of at least 2 mm was clearly demonstrated in a cell + NPs exposure test. We finally applied this probe in a TiO_2 NP-induced cytotoxicity assay. Results revealed a concentration/time dependence of the NP's cytotoxicity. Results

also demonstrated the probe's potential for fast, local and continuous monitoring of cellular events in a staining-free manner, which may greatly impact future quasi-single-cell and cell-heterogeneity-driven researches.

Acknowledgments

The authors would like to thank Clarissa A. Wisner and Qianyao Li at the Missouri University of Science and Technology, for their assistance with SEM imaging and EDS scanning. The authors also thank Dr. Kathleen Browne for her proof-reading and editing assistance for this manuscript. This work was supported by the National Institute of Health (NIH, 1R21GM104696-01).

References

1. Arriaga EA. Single cell heterogeneity. Single Cell Analysis: Technologies and Applications. 2009:223–34.
2. Aird WC. Endothelial cell heterogeneity. Critical care medicine. 2003; 31:S221–S30. [PubMed: 12682444]
3. Tang DG. Understanding cancer stem cell heterogeneity and plasticity. Cell research. 2012; 22:457–72. [PubMed: 22357481]
4. Altschuler SJ, Wu LF. Cellular heterogeneity: do differences make a difference? Cell. 2010; 141:559–63. [PubMed: 20478246]
5. Davey HM, Kell DB. Flow cytometry and cell sorting of heterogeneous microbial populations: the importance of single-cell analyses. Microbiological reviews. 1996; 60:641–96. [PubMed: 8987359]
6. Elowitz MB, Levine AJ, Siggia ED, Swain PS. Stochastic gene expression in a single cell. Science. 2002; 297:1183–6. [PubMed: 12183631]
7. Kamme F, Salunga R, Yu J, Tran D-T, Zhu J, Luo L, et al. Single-cell microarray analysis in hippocampus CA1: demonstration and validation of cellular heterogeneity. The Journal of neuroscience. 2003; 23:3607–15. [PubMed: 12736331]
8. Casey JR, Grinstein S, Orlowski J. Sensors and regulators of intracellular pH. Nature reviews Molecular cell biology. 2010; 11:50–61. [PubMed: 19997129]
9. Haas A. The phagosome: compartment with a license to kill. Traffic. 2007; 8:311–30. [PubMed: 17274798]
10. Kurkdjian A, Guern J. Intracellular pH: measurement and importance in cell activity. Annual review of plant biology. 1989; 40:271–303.
11. Webb BA, Chimenti M, Jacobson MP, Barber DL. Dysregulated pH: a perfect storm for cancer progression. Nature Reviews Cancer. 2011; 11:671–7. [PubMed: 21833026]
12. Neri D, Supuran CT. Interfering with pH regulation in tumours as a therapeutic strategy. Nature reviews Drug discovery. 2011; 10:767–77. [PubMed: 21921921]
13. Matés JM, Segura JA, Alonso FJ, Márquez J. Intracellular redox status and oxidative stress: implications for cell proliferation, apoptosis, and carcinogenesis. Archives of toxicology. 2008; 82:273–99. [PubMed: 18443763]
14. Chiche J, Ilc K, Laferrière J, Trottier E, Dayan F, Mazure NM, et al. Hypoxia-inducible carbonic anhydrase IX and XII promote tumor cell growth by counteracting acidosis through the regulation of the intracellular pH. Cancer research. 2009; 69:358–68. [PubMed: 19118021]
15. Gillies RJ, Raghunand N, Karczmar GS, Bhujwalla ZM. MRI of the tumor microenvironment. Journal of Magnetic Resonance Imaging. 2002; 16:430–50. [PubMed: 12353258]
16. Busco G, Cardone RA, Greco MR, Bellizzi A, Colella M, Antelmi E, et al. NHE1 promotes invadopodial ECM proteolysis through acidification of the peri-invadopodial space. The FASEB Journal. 2010; 24:3903–15. [PubMed: 20547664]
17. Han J, Burgess K. Fluorescent indicators for intracellular pH. Chemical reviews. 2009; 110:2709–28.
18. Booth IR. The regulation of intracellular pH in bacteria, Novartis Foundation Symposium 221-Bacterial Responses to Ph. Wiley Online Library. 2007:19–37.

19. Martin C, Pedersen SF, Schwab A, Stock C. Intracellular pH gradients in migrating cells. American Journal of Physiology-Cell Physiology. 2011; 300:C490–C5. [PubMed: 21148407]
20. Roos, A., Boron, WF. Intracellular pH: Am Physiological Soc. 1981.
21. Minton K. Cell signalling: Responding to intracellular pH. Nature Reviews Molecular Cell Biology. 2013; 14:608–9.
22. LIU J, DIWU Z, KLAUBERT D. Fluorescent Molecular Probes. Part 3. 2′, 7′-Bis-(3-carboxypropyl)-5-(and-6)-carboxyfluorescein (BCPCF): A New Polar Dual-Excitation and Dual-Emission pH Indicator with a PKA of 7.0. ChemInform. 1998; 29
23. Benjaminsen RV, Sun H, Henriksen JR, Christensen NM, Almdal K, Andresen TL. Evaluating nanoparticle sensor design for intracellular pH measurements. ACS nano. 2011; 5:5864–73. [PubMed: 21707035]
24. Peng J, He X, Wang K, Tan W, Wang Y, Liu Y. Noninvasive monitoring of intracellular pH change induced by drug stimulation using silica nanoparticle sensors. Analytical and bioanalytical chemistry. 2007; 388:645–54. [PubMed: 17440714]
25. Ruedas-Rama MJ, Walters JD, Orte A, Hall EA. Fluorescent nanoparticles for intracellular sensing: a review. Analytica chimica acta. 2012; 751:1–23. [PubMed: 23084048]
26. Dennis AM, Rhee WJ, Sotto D, Dublin SN, Bao G. Quantum dot–fluorescent protein FRET probes for sensing intracellular pH. ACS nano. 2012; 6:2917–24. [PubMed: 22443420]
27. Toumazou C, Purushothaman S. Use of a pH sensor comprising an ion-sensitive field effect transistor (ISFET) to perform real time detection/quantification of nucleic acid amplification. Google Patents. 2012
28. Sakurai T, Husimi Y. Real-time monitoring of DNA polymerase reactions by a micro ISFET pH sensor. Analytical chemistry. 1992; 64:1996–7. [PubMed: 1416046]
29. Udd, E., Spillman, WB, Jr. Fiber optic sensors: an introduction for engineers and scientists. John Wiley & Sons; 2011.
30. Froggatt M, Moore J. High-spatial-resolution distributed strain measurement in optical fiber with Rayleigh scatter. Applied Optics. 1998; 37:1735–40. [PubMed: 18273081]
31. Reed WA, Yan MF, Schnitzer MJ. Gradient-index fiber-optic microprobes for minimally invasive in vivo low-coherence interferometry. Optics letters. 2002; 27:1794–6. [PubMed: 18033366]
32. Vo-Dinh T, Kasili P. Fiber-optic nanosensors for single-cell monitoring. Analytical and bioanalytical chemistry. 2005; 382:918–25. [PubMed: 15928944]
33. Chaudhury N, Gupta R, Gulia S. Sol-gel Technology for Sensor Applications (Review Paper). Defence Science Journal. 2007; 57:241–53.
34. Lin J, Brown CW. Sol-gel glass as a matrix for chemical and biochemical sensing. TrAC Trends in Analytical Chemistry. 1997; 16:200–11.
35. Yang Q, Wang H, Lan X, Cheng B, Chen S, Shi H, et al. Reflection-mode micro-spherical fiber-optic probes for in vitro real-time and single-cell level pH sensing. Sensors and Actuators B: Chemical. 2015; 207:571–80.
36. Yang Q, Wang H, Chen S, Lan X, Xiao H, Shi H, et al. Fiber-Optic-Based Micro-Probe Using Hexagonal, 1-in-6 Fiber Configuration for Intracellular Single-Cell pH Measurement. Analytical chemistry. 2015; 87:7171–9. [PubMed: 26118725]
37. Yang Q, Wang H, Chen S, Lan X, Xiao H, Shi H, et al. A Novel Fiber-Optic Based Micro-Probe Using Hexagonal 1-in-6 Fiber Configuration for Intracellular Single-Cell pH Measurement. Analytical chemistry. 2015
38. Agasti SS, Rana S, Park M-H, Kim CK, You C-C, Rotello VM. Nanoparticles for detection and diagnosis. Advanced drug delivery reviews. 2010; 62:316–28. [PubMed: 19913581]
39. Hahn MA, Singh AK, Sharma P, Brown SC, Moudgil BM. Nanoparticles as contrast agents for in-vivo bioimaging: current status and future perspectives. Analytical and bioanalytical chemistry. 2011; 399:3–27. [PubMed: 20924568]
40. Brannon-Peppas L, Blanchette JO. Nanoparticle and targeted systems for cancer therapy. Advanced drug delivery reviews. 2012; 64:206–12.
41. Cho K, Wang X, Nie S, Shin DM. Therapeutic nanoparticles for drug delivery in cancer. Clinical cancer research. 2008; 14:1310–6. [PubMed: 18316549]

42. Pradeep T. Noble metal nanoparticles for water purification: a critical review. Thin solid films. 2009; 517:6441–78.
43. Bolzinger MA, Briançon S, Chevalier Y. Nanoparticles through the skin: managing conflicting results of inorganic and organic particles in cosmetics and pharmaceutics. Wiley Interdisciplinary Reviews: Nanomedicine and Nanobiotechnology. 2011; 3:463–78. [PubMed: 21618448]
44. Wiechers JW, Musee N. Engineered inorganic nanoparticles and cosmetics: facts, issues, knowledge gaps and challenges. Journal of biomedical nanotechnology. 2010; 6:408–31. [PubMed: 21329039]
45. Chen J, Dong X, Zhao J, Tang G. In vivo acute toxicity of titanium dioxide nanoparticles to mice after intraperitioneal injection. Journal of Applied Toxicology. 2009; 29:330–7. [PubMed: 19156710]
46. Park E-J, Yi J, Chung K-H, Ryu D-Y, Choi J, Park K. Oxidative stress and apoptosis induced by titanium dioxide nanoparticles in cultured BEAS-2B cells. Toxicology letters. 2008; 180:222–9. [PubMed: 18662754]
47. Shukla RK, Sharma V, Pandey AK, Singh S, Sultana S, Dhawan A. ROS-mediated genotoxicity induced by titanium dioxide nanoparticles in human epidermal cells. Toxicology in Vitro. 2011; 25:231–41. [PubMed: 21092754]
48. Vistica DT, Skehan P, Scudiero D, Monks A, Pittman A, Boyd MR. Tetrazolium-based assays for cellular viability: a critical examination of selected parameters affecting formazan production. Cancer Research. 1991; 51:2515–20. [PubMed: 2021931]
49. Love SA, Maurer-Jones MA, Thompson JW, Lin Y-S, Haynes CL. Assessing nanoparticle toxicity. Annual review of analytical chemistry. 2012; 5:181–205.
50. Kowaltowski AJ, de Souza-Pinto NC, Castilho RF, Vercesi AE. Mitochondria and reactive oxygen species. Free Radical Biology and Medicine. 2009; 47:333–43. [PubMed: 19427899]
51. Matsuyama S, Reed J. Mitochondria-dependent apoptosis and cellular pH regulation. Cell death and differentiation. 2000; 7:1155–65. [PubMed: 11175252]

Biographies

Sisi Chen is a graduate student in Chemistry Department at Missouri University of Science and Technology. She received her BS degree in school of chemical biology and pharmaceutical sciences at Capital Medical University in 2012 in Beijing, China. She joined Dr. Yinfa Ma's research group in 2012 and her research interests including analytical chemistry and bioactive material characterization and evaluation. She is currently focusing on micro-sized fiber-optic probe development for bioanalysis. Efforts has also been put into the wound healing mechanism study of different types of bioactive glass nanofibers as well as cancer biomarker analysis using UPLC-MS/MS system.

Qingbo Yang received his BS degree in Department of Bio-Engineering at Zhengzhou University in China, and MS in molecular biology and biochemistry from Shanghai University in China. He joined Dr. Yinfa Ma's group since September, 2010, and his research interests emphasized on nanomaterial safety and cytotoxicity, single cell and single molecule level imaging and analysis. He is currently working as research assistant in Chemistry Department and the Center for Single Nanoparticles, Single Cell and Single Molecules Monitoring (CS^3M) at Missouri University of Science and Technology.

Hai Xiao received his PhD in electrical engineering from Virginia Tech in 2000. He is the Samuel Lewis Bell Distinguished Professor of Electrical and Computer Engineering, jointly affiliated with COMSET, at Clemson University. His research interests mainly focus on

photonic and microwave sensors and instrumentation for applications in energy, intelligent infrastructure, clean-environment, biomedical sensing/imaging, and national security.

Honglan Shi received her PhD in analytical chemistry from Missouri University of Science and Technology in May, 2010. She is an associate research professor in Department of Chemistry at Missouri University of Science and Technology. Her research mainly focus on development of advanced analytical techniques and methods for bioanalytical and environmental applications including state-of-the-art instrument development and manufacturing, bioactive glass-biofluid-bioorganism interaction study by advance analytical technologies, advanced test kit developments and manufacturing, method development for rapid characterization and quantification of engineered nanomaterials, development of novel economical and green technologies for water treatment, development of trace emerging pollutants analysis and control in natural and drinking water.

Yinfa Ma received his PhD in analytical chemistry and minor PhD in biochemistry from Iowa State University. He is a Curators' Teaching Professor in Department of Chemistry at Missouri University of Science and Technology. His research focuses on bio-analysis and bio-separations, environmental monitoring, and single molecule and single cell imaging, by using variety of state-of-art instruments, such as high performance liquid chromatography (HPLC), high performance capillary electrophoresis (HPCE), GC–MS, HPLC–MS, HPCE–MS, gel electrophoresis, size-exclusion chromatography, and home-built single molecule and single cell imaging system.

Research Highlights

- A miniaturized micro-probe was fabricated for monitoring the pHs in a niche cellular environment;
- Novel designed dual-core double-fiber configuration efficiently enhanced S/N ratio;
- Fast probe fabrication through a gravitational-stretching system and OrMoSil dip-coating technique;
- Acquire pH resolution of 0.035 ± 0.005 pH units within a biological relevant range of 6.20 – 7.92;
- Detecting early onset of cell deterioration induced by TiO_2 nanoparticles on A549 cells.

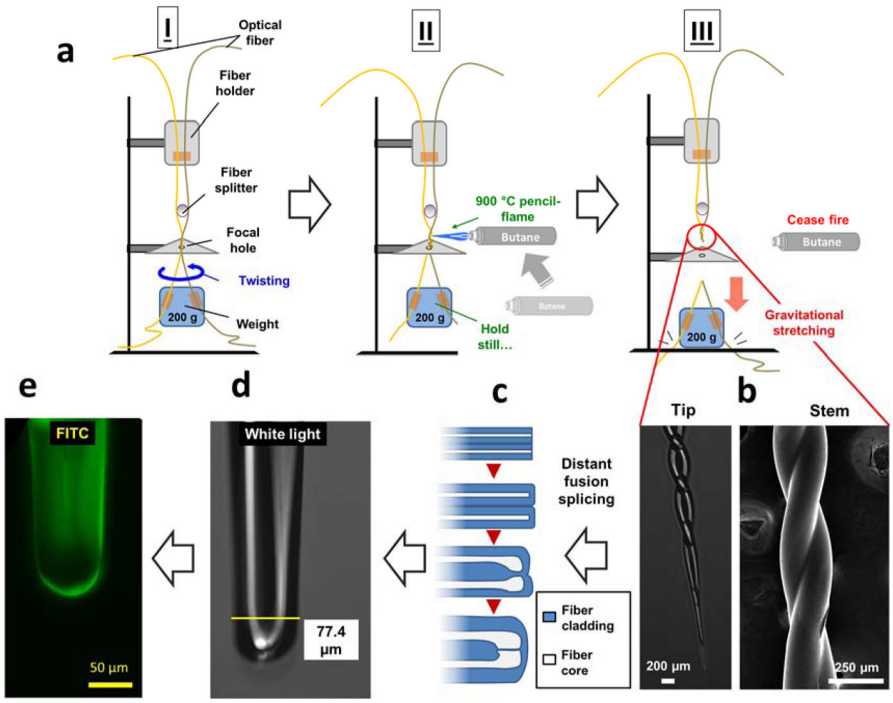

Figure 1.

Procedures of fabricating dual-core twisted micro-pH probe. a) Fabrication of the probe stem by double-fiber twisting and gravitational-stretching using a home-built device; b) SEM and inverted microscopic images of fabricated probe stem and tip; c) schemes of how to fuse paralleled tapered fiber tips into the final dual core configuration using distant fusion splicing method; d) inverted microscopic image of fabricated dual core probe tip under white light; e) fabricated probe tip image under Fluorescein isothiocyanate (FITC) channel.

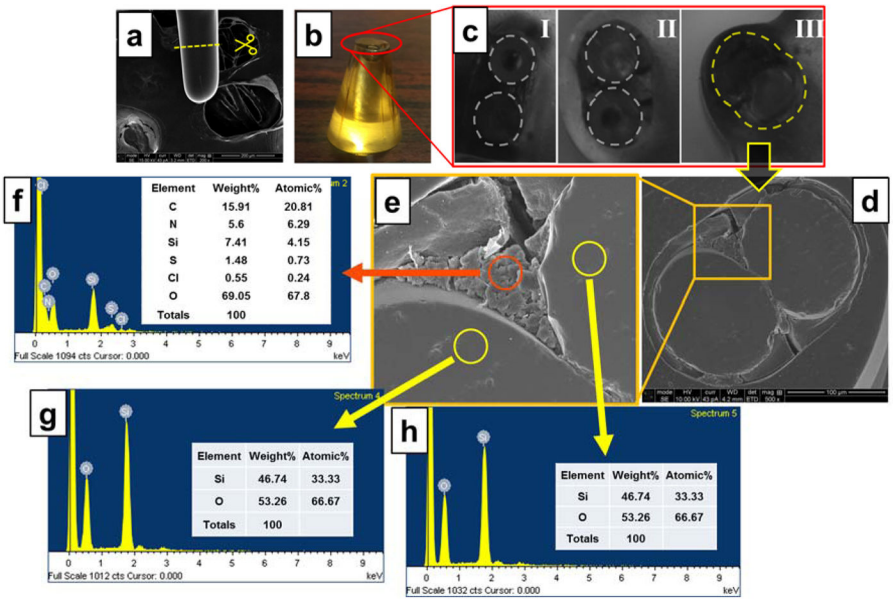

Figure 2.

Probe characterization by SEM and EDS analysis. a) SEM image of probe tip; b) the epoxy module immobilized several finished probe within it; c) three different probe cross-sections; d) SEM image of cross section of the dual-core double-fiber twisted pH probe; e) magnified image of square area in (d); f) EDS scanning result of red-circled area in (e); g) and h) EDS scanning results of yellow-circled areas in (e).

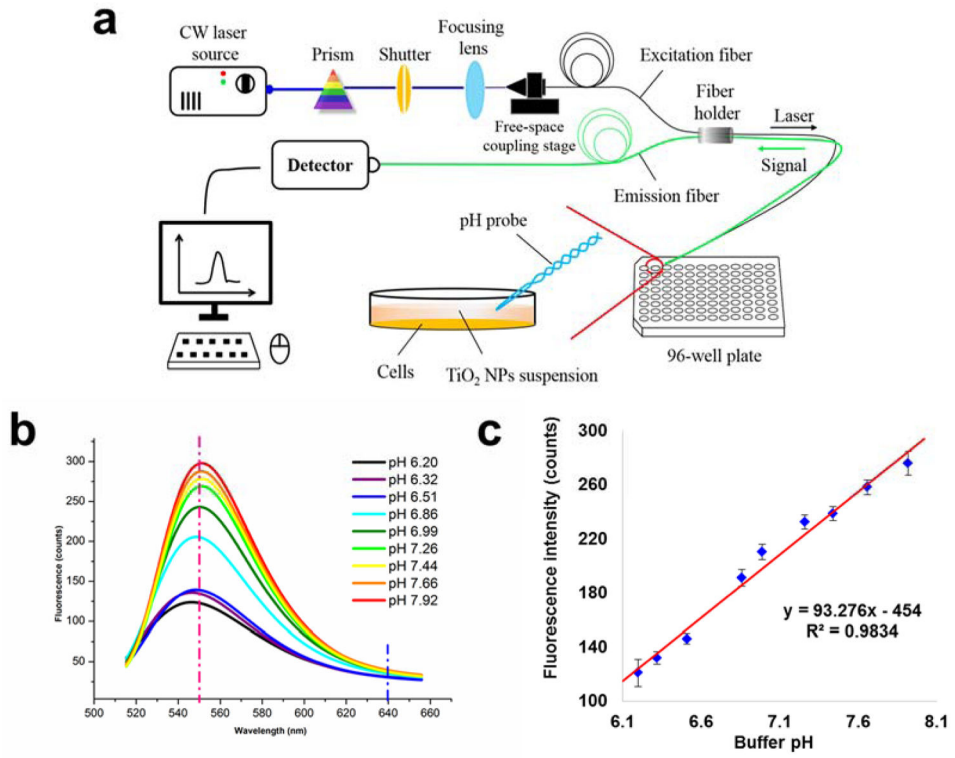

Figure 3.

a) Schematic diagram of system setup. The integrated system consisted of a CW Argon laser source, a prism, a shutter, a focusing lens, a free-space coupling stage, a detector, and a computer. The dual-core double-fiber twisted pH probe was integrated into the system and was applied for pH measurements in each well of a 96-well plate; b) A fluorescent spectra was plotted based on probe signal intensity range from 510 nm to 650 nm under a set of standardized pH buffer solution that ranged from pH 6.20 to pH 7.92. The vertical red and blue dash lines represent the peak (550 nm) wavelength and the reference wavelength (640 nm) for final ratio-based pH calculation (I_{550nm}/I_{640nm}); c) Linear correlation between buffer pH and fluorescent spectra peak intensity.

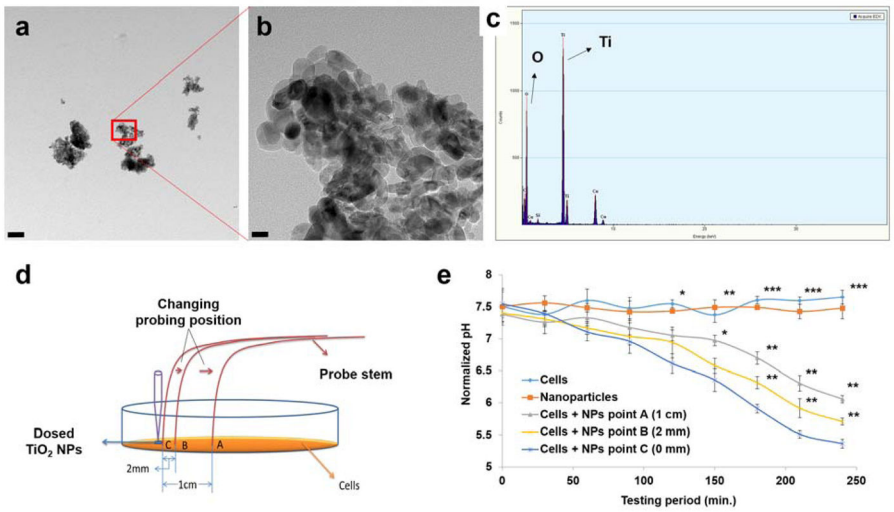

Figure 4.

TiO_2 NPs characterization and determination of the probe's spatial resolution. a) TEM image of applied TiO_2 NPs, and b) zoom-in image of the NPs squared in a). c) EDS scanning result showing chemical composition of the TiO_2 NPs. d) Schematic of how to test the spatial resolution of the pH micro-probe. E) Four-hour continual pH monitoring of cells + NP response at three different spots as shown in d), and compared with cell-only and NP-only groups. Statistical significance is interpreted as a *p*-value of <0.05 (*), <0.01 (**) as well as <0.001 (***). Scale bar: a) 200 nm; b) 20 nm.

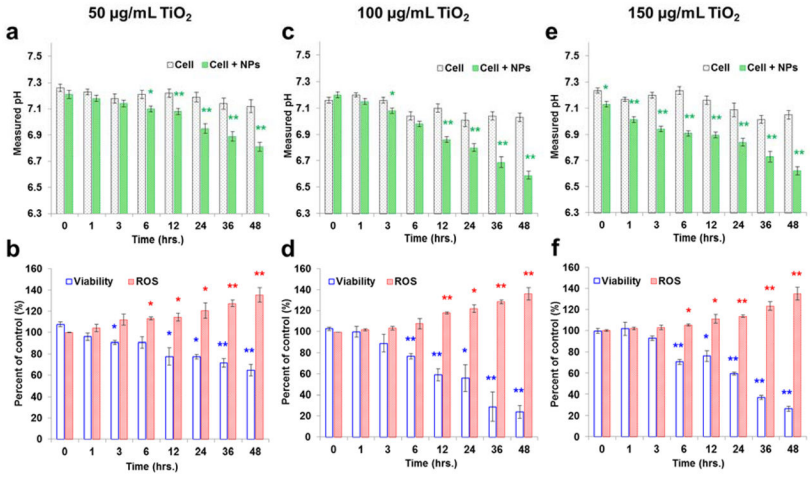

Figure 5.

The application of the novel pH probe in measuring cell colony's pH variations and their comparison d with cell viability and ROS generation in a TiO_2 NP-induced cytotoxicity model. Green plots are pH measurement using our developed probe, blue and red plots are data are the cell viability and ROS kits measurements. Three NP concentration, 50, 100 and 150 μg/mL, were used is this study. Values are mean ± SD (n≥3). Statistical significance was indicated by $*p < 0.05$ (significant), and $** p < 0.01$ (very significant), versus the control groups.